Geophysical Research Letters

RESEARCH LETTER
10.1029/2020GL087736

On the Role of Pacific-Atlantic SST Contrast and Associated Caribbean Sea Convection in August–October U.S. Regional Rainfall Variability

Dongmin Kim[1,2], Sang-Ki Lee[2], Hosmay Lopez[2], Gregory R. Foltz[2], Vasubandhu Misra[3], and Arun Kumar[4]

[1]Cooperative Institute for Marine and Atmospheric Studies, University of Miami, Miami, FL, USA, [2]Atlantic Oceanographic and Meteorological Laboratory, NOAA, Miami, FL, USA, [3]Center for Ocean-Atmospheric Prediction Studies, Florida State University, Tallahassee, FL, USA, [4]Climate Prediction Center, NOAA, College Park, MD, USA

Key Points:
- This study investigates the large-scale atmospheric conditions that modulate U.S. rainfall variability in August–October
- The well-recognized relationship between NASH and U.S. rainfall in peak summer is not applicable in August–October
- Earlier key findings are integrated to link the Pacific-Atlantic SST contrast, Caribbean Sea convection, and U.S. rainfall in ASO

Supporting Information:
- Supporting Information SI

Correspondence to:
D. Kim,
dongmin.kim@noaa.gov

Citation:
Kim, D., Lee, S.-K., Lopez, H., Foltz, G. R., Misra, V., & Kumar, A. (2020). On the role of Pacific-Atlantic SST contrast and associated Caribbean Sea convection in August–October U.S. regional rainfall variability. *Geophysical Research Letters*, *47*, e2020GL087736. https://doi.org/10.1029/2020GL087736

Received 28 FEB 2020
Accepted 10 MAY 2020
Accepted article online 16 MAY 2020

Abstract This study investigates the large-scale atmospheric processes that lead to U.S. precipitation variability in late summer to midfall (August–October; ASO) and shows that the well-recognized relationship between North Atlantic Subtropical High and U.S. precipitation in peak summer (June–August) significantly weakens in ASO. The working hypothesis derived from our analysis is that in ASO convective activity in the Caribbean Sea, modulated by the tropical Pacific-Atlantic sea surface temperature (SST) anomaly contrast, directly influences the North American Low-Level Jet and thus U.S. precipitation east of the Rockies, through a Gill-type response. This hypothesis derived from observations is strongly supported by a long-term climate model simulation and by a linear baroclinic atmospheric model with prescribed diabatic forcings in the Caribbean Sea. This study integrates key findings from previous studies and advances a consistent physical rationale that links the Pacific-Atlantic SST anomaly contrast, Caribbean Sea convective activity, and U.S. rainfall in ASO.

Plain Language Summary This study investigates the large-scale atmospheric processes that modulate U.S. rainfall variability in late summer to midfall (August–October; ASO). We show that the well-recognized relationship between the Bermuda High and U.S. rainfall in peak summer (June–August) is not applicable in ASO. Instead, both observations and model simulations show that in ASO atmospheric convective activity in the Caribbean Sea, modulated by the Pacific-Atlantic interbasin sea surface temperature (SST) anomaly contrast, directly influences the atmospheric low-level jet that carries warm and moist air from the Gulf of Mexico into the United States and thus affects U.S. rainfall variability. This study integrates key findings from previous studies and advances a consistent physical rationale that links the Pacific-Atlantic SST anomaly contrast, Caribbean Sea convective activity, and U.S. rainfall in ASO.

1. Introduction

Understanding the physical mechanisms controlling U.S. summer to midfall (June–October) precipitation variability is of great importance due to its impacts on the spatiotemporal variation of extreme events, including drought, flooding, and heat waves, and on agricultural productivity. Thus, it is imperative to study the potential drivers of precipitation variability to improve their prediction. Previous studies have explored physical links between U.S. summer to midfall precipitation and climate variations at various time scales (e.g., McCabe et al., 2004; Schubert et al., 2009; Wei et al., 2019). Some studies (e.g., Krishnamurthy et al., 2015; Mo & Schemm, 2008; Seager, 2007; Weaver et al., 2009) have shown that tropical Pacific sea surface temperature anomalies (SSTAs) can modulate U.S. precipitation variability in boreal summer via Walker circulation changes. For instance, Weaver et al. (2009) and Krishnamurthy et al. (2015) emphasized that interannual variation of the North American Low-Level Jet (NALLJ), a key driver of U.S. warm season (April–September) rainfall variability, could be modulated by tropical Pacific SSTAs in midsummer to early fall (July–September). Mo et al. (2009) also showed that the decadal frequency of U.S. drought in midsummer to early fall is significantly influenced by tropical Pacific SSTAs, while the direct influence of Atlantic SSTAs is relatively small.

Other studies, however, have suggested that Atlantic warm pool (AWP) variability and associated SSTAs in the Gulf of Mexico (GoM), Caribbean Sea (CS), and western tropical North Atlantic could serve as main drivers of U.S. summer to midfall precipitation variability, especially over the southern United States at interannual (e.g., Wang et al., 2006, 2008; Wang & Lee, 2007; Misra et al., 2011; Misra & Li, 2014; Liu et al., 2015) and decadal time scales (e.g., Curtis, 2008; Enfield et al., 2001; Hu et al., 2011; Hu & Feng, 2008; McCabe et al., 2004; Nigam et al., 2011; Schubert et al., 2009; Sutton & Hodson, 2005). These studies suggested that at both interannual and decadal time scales warm AWP SSTAs (i.e., larger-than-normal AWP) can decrease precipitation over the southern United States and vice versa for cold AWP SSTAs. Almost all of these studies invoke a well-recognized relationship that warm AWP SSTAs weaken the North Atlantic Subtropical High (NASH) and thus displace the western leg of the NASH eastward and away from the eastern U.S. seaboard. This shift in the NASH weakens the NALLJ and thus reduces the supply of warm and moist air from the GoM into the United States (e.g., Algarra et al., 2019; Arias et al., 2012; Bishop et al., 2019; Curtis, 2008; Feng et al., 2011; Hu et al., 2011; Hu & Feng, 2008; Hu & Feng, 2012; Li et al., 2011; Liu et al., 2015; Mo et al., 2009; Schubert et al., 2009; Sutton & Hodson, 2005; Wang et al., 2006).

As briefly summarized above, the variation of summer to midfall U.S. precipitation could be a response to complex interactions between the tropical Pacific and AWP SSTAs and their influence on NASH. However, there are several remaining key questions regarding the connections between tropical Pacific and AWP SSTAs and their impacts on U.S. summer to midfall precipitation variability. Particularly, NASH in late summer to midfall (August–October; ASO) is substantially weaker than in peak summer (June–August; JJA) and does not extend as far westward to influence NALLJ (e.g., Song et al., 2018a, 2018b), as shown in Figure 1. However, the AWP and its impact on the atmosphere aloft and Atlantic tropical cyclone activity are strongest in ASO (e.g., Lee et al., 2007; Wang et al., 2006; Wang & Enfield, 2001). Therefore, the underlying physical mechanism linking the AWP SSTAs to U.S. precipitation in ASO needs to be clarified. It is also not entirely clear through what mechanism U.S. precipitation in ASO and associated atmospheric circulation features are remotely forced by tropical Pacific SSTAs.

The main goals of this study are to investigate the relationship between tropical Pacific-Atlantic SSTAs and U.S. precipitation during ASO and to explore the underlying physical mechanisms (sections 3 and 4). Based on our analysis of observational and atmospheric reanalysis data sets, we hypothesize that convective activity over the CS is largely influenced by the tropical Pacific and Atlantic SST contrast and that this is a key process in modulating U.S. precipitation in ASO (section 5). We further use a long-term climate model simulation and a simple linear baroclinic atmospheric model (LBM) with prescribed diabatic forcing to test and validate this hypothesis (section 6).

2. Data, Methods, and Models

We use National Oceanic and Atmospheric Administration (NOAA)'s interpolated outgoing longwave radiation (OLR; Liebmann & Smith, 1996) and Extended Reconstructed SST version 5 (ERSST5; Huang et al., 2017) to explore the relationship between convective activity over the CS and global SSTAs. Monthly precipitation fields are derived from Climatic Research Unit (CRU) version 3.2 climate data (Jones & Harris, 2013). The National Centers for Environmental Prediction reanalysis version 2 (NCEP2; Kanamitsu et al., 2002) is used to derive monthly atmospheric circulation fields. The study period is from 1979 to 2018 (40 years). To minimize the potential impact of anthropogenic global warming, all variables are linearly detrended.

We use a 1,100 model year simulation of the Community Earth System Model-Large Ensemble Simulation (CESM-LENS) with a constant preindustrial CO_2 level (Kay et al., 2015) in order to test our results and hypotheses derived from the observational and reanalysis data sets. We also use a LBM (Watanabe & Kimoto, 2000) to explore the atmospheric dynamics linking CS convective activity and U.S. summer precipitation. The LBM is a useful tool for diagnosing anomalous atmospheric circulations forced by regional diabatic heating or Rossby wave sources (e.g., Lee et al., 2009; Lopez et al., 2019; Ting & Wang, 1997; Watanabe & Kimoto, 2000). The LBM configured for this work has a T21 horizontal resolution (~5° × 5°) and five vertical levels in a sigma coordinate (T21L5).

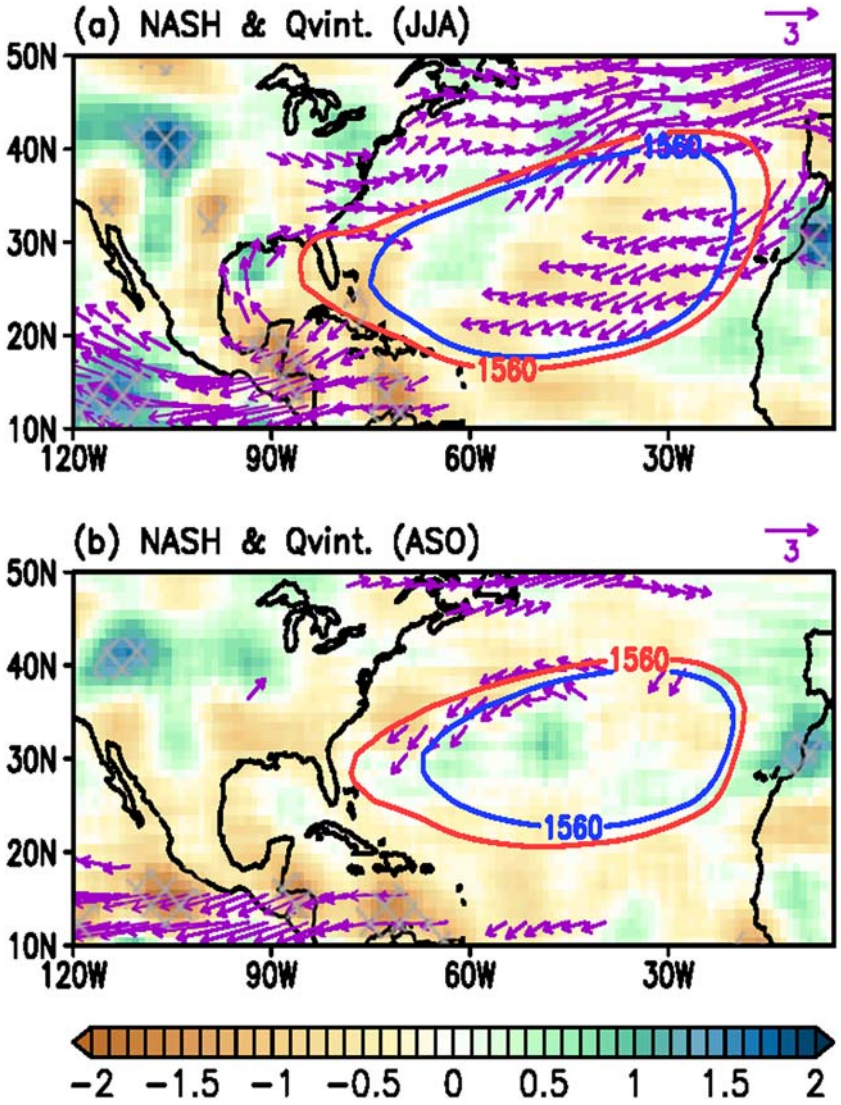

Figure 1. Differences in vertically integrated moisture convergence (shaded, 10^{-8} kg m^{-2} s^{-1}, hatched regions are statistically significant at the 95% level) and fluxes (vectors, 10^{-8} kg m^{-1} s^{-1}, omitted if less than 10^{-8} kg m^{-1} s^{-1}) between strong and weak NASH years during (a) June-July-August (JJA) and (b) August-September-October (ASO). The strong (13 years) and weak (11 years) NASH years are selected when the spatially averaged (80–30°W, 20–40°N) geopotential height at 850 hPa is larger than one standard deviation above the mean and smaller than one standard deviation below the mean, respectively. Red and blue lines are the edge of NASH (1,560 gpm) in the strong NASH and weak NASH years, respectively.

3. Relationship Between NASH and U.S. Precipitation

In this section, we revisit the relationship between NASH and U.S. summer precipitation by performing a composite analysis using NCEP2 reanalysis. First, the strength of NASH is identified by the 850 hPa geopotential heights averaged over 80–30°W and 20–40°N for both JJA and ASO seasons. Then, we select strong and weak NASH years with their amplitudes of positive and negative anomalies larger than the standard deviation. We find 13 strong NASH years and 11 weak NASH years for JJA and ASO (Figure 1). Note that the strong and weak years for JJA are not necessarily the same years for ASO. Following Wei et al. (2019), the 1,560 geopotential height (gpm) isoline at 850 hPa is used to represent the spatial extent of NASH.

The western leg of NASH extends toward the southeast United States in the strong NASH composite but remains over the Atlantic Ocean off the eastern U.S. seaboard in the weak NASH composite in JJA

(Figure 1a). Accordingly, the composite differences (i.e., strong − weak NASH years) of vertically integrated moisture flux and convergence increase over the south and southeast United States in JJA. During ASO, however, the western leg of NASH resides largely within the Atlantic Ocean without reaching the eastern U.S. seaboard in both strong and weak NASH composites (Figure 1b). Consistently, the composite differences of vertically integrated moisture flux and convergence over the United States are much smaller in ASO compared to JJA. Hence, the U.S. precipitation difference averaged over the central and eastern United States (90–70°W, 30–40°N) is much smaller in ASO (0.02 mm day^{-1}) compared to JJA (0.34 mm day^{-1}). These results suggest that climatologically, NASH is strong enough in JJA to significantly modulate U.S. precipitation, but in ASO it is farther away from the eastern United States and thus difficult to influence U.S. precipitation directly.

4. Pacific-Atlantic Interbasin SSTA Contrast and U.S. Precipitation in ASO

In this section, we first explore the relationship between U.S. precipitation and global SSTAs in ASO. Tropical Pacific SSTAs north of the equator (160°E to 160°W, 0–20°N) have a strong positive correlation with U.S. precipitation east of the Rockies (90–70°W, 30–40°N, Figure 2a). In contrast, SSTAs over the Atlantic warm pool (AWP; 80–40°W, 10–25°N) and South China Sea (SCS; 110–130°E, 10–40°N) have strong negative correlations with U.S. precipitation. Specifically, the U.S. rainfall correlation with AWP SSTAs and tropical Pacific SSTAs (PAC; 160°E to 160°W, 0–10°N) are −0.35 and 0.31, respectively, both of which are statistically significant at the 95% level based on a Student's *t* test (supporting information Table S1). There is also significant negative correlation with SSTAs in the SCS (110–130°E, 10–40°N). These correlations are much weaker and statistically insignificant in JJA (Figure S1 and Table S2).

Note that the tropical Pacific SSTAs and AWP SSTAs are uncorrelated ($r = -0.01$), indicating that SSTAs in the two regions are statistically independent from one another (e.g., Wang et al., 2008). Therefore, we develop a Pacific-Atlantic interbasin SSTA index, defined as the difference in SSTAs between the PAC and AWP regions (Figure 2a). As expected, this interbasin SSTA index is correlated with U.S. precipitation in ASO ($r = 0.39$; Figure 2b). These significant correlations suggest that the Pacific-Atlantic interbasin SSTA contrast modulates the Walker circulation and in turn changes tropical convective activity over the tropical Pacific and Atlantic (e.g., Bjerknes, 1969; Wang et al., 2017). Consistent with this line of reasoning, the interbasin SSTA index and OLR anomalies are correlated in the tropical Pacific, the CS (90–70°W, 10–20°N), and the SCS (Figure 2b), in agreement with the spatial pattern of correlation coefficients between tropical SSTAs and U.S. precipitation (Figure 2a).

A number of studies have shown that CS precipitation is strongly influenced by the interaction between the AWP and eastern tropical Pacific SSTAs (e.g., Enfield & Alfaro, 1999; Giannini et al., 2000, 2001; Spence et al., 2004). More specifically, it is well recognized that warm eastern tropical Pacific and cold AWP SSTAs produce anomalous subsidence over the CS and thus decrease CS precipitation. Additionally, several studies have shown that El Niño-like patterns in the Pacific can decrease convective activity over the CS via the Walker circulation (e.g., Krishnamurthy et al., 2015; Weaver et al., 2009). The physical mechanism underlying the relationship between warm central Pacific SSTAs (i.e., El Niño-like pattern) and anomalous subsidence over the tropical Atlantic has been shown in previous studies. As discussed in Chiang and Sobel (2002), Lintner and Chiang (2007), and other studies, warm SSTAs over the central tropical Pacific (i.e., El Niño-like) induce tropospheric warming over the global tropics via fast Kelvin wave propagation, which in turn increases atmospheric stability and thus promotes anomalous subsidence over the AWP region. Cold AWP SSTAs further reinforce the increased atmospheric stability aloft (i.e., colder atmosphere at low-level and warmer atmosphere at upper level). This mechanism is well supported by the anomalous ascending motion in the central tropical Pacific and descending motion in the western tropical Atlantic, linked to the suppressed CS convection (Figure 2c). This is also consistent with the suppressed OLR anomalies over the CS in response to warm Pacific SSTAs and cold AWP SSTAs from the partial correlation analysis (Figure S2). Therefore, the correlation between the interbasin SSTA index and OLR anomalies over the CS is significantly high ($r = 0.63$; Table S1). But, more importantly, the correlation between the CS OLR anomalies and U.S. precipitation is also high ($r = 0.45$; Table S1). These results clearly illustrate that tropical Pacific and Atlantic SSTAs modulate U.S. precipitation during ASO through their combined impact (i.e., interbasin SSTA contrast) on CS convective activity.

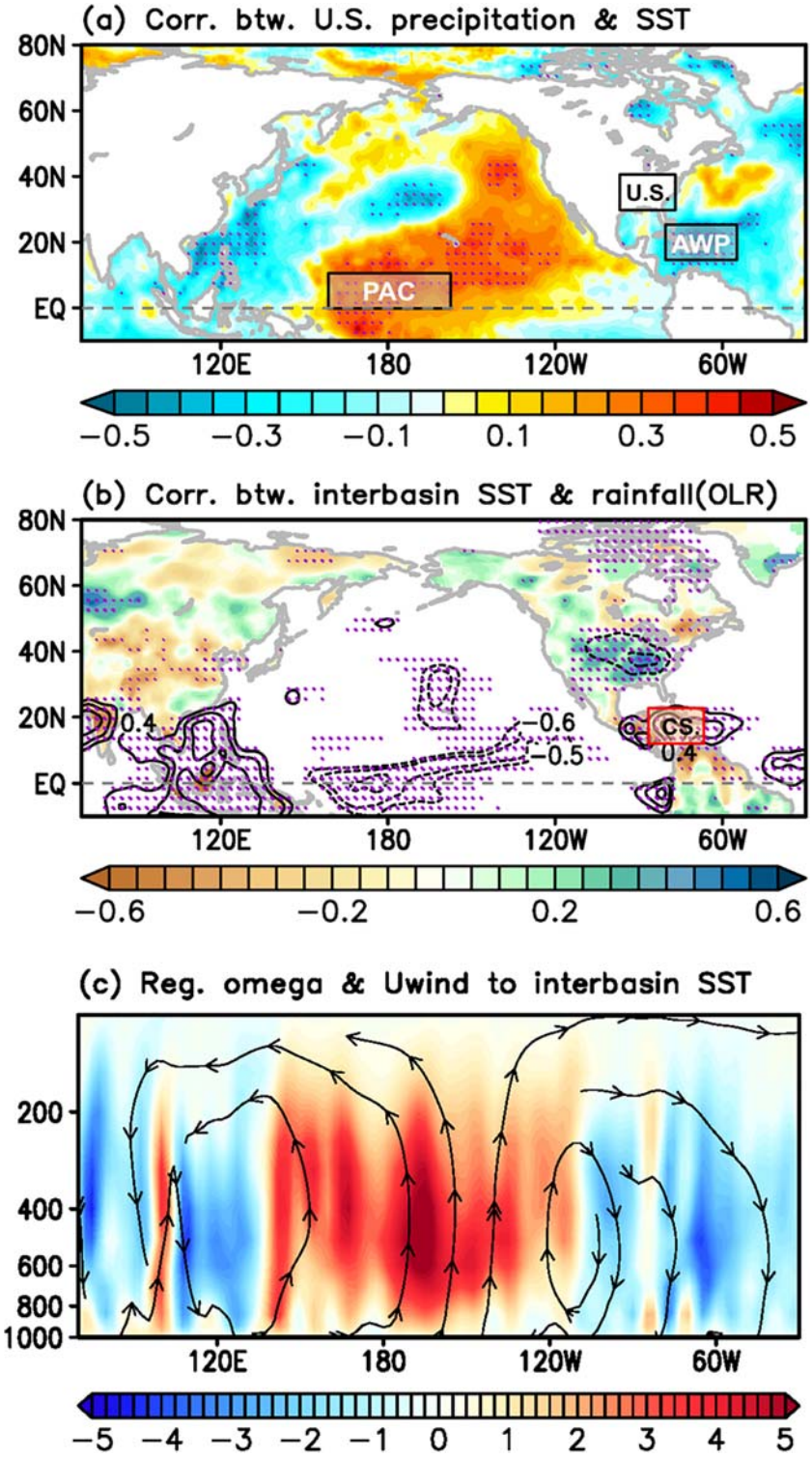

Figure 2. (a) Correlation between U.S. precipitation (90–70°W, 30–40°N) and SSTAs in ASO for 40 years (1979–2018). (b) Correlation between interbasin SSTA contrast and OLR anomalies in ASO (contours) and between interbasin SSTA contrast and land precipitation in ASO (shaded). The interbasin SSTA contrast is defined as the difference in SSTAs between the tropical Pacific (PAC; 160°E to 160°W, 0–10°N) and Atlantic warm pool (AWP; 80–40°W, 10–25°N) regions. Purple dotted areas in (b) indicate correlation between interbasin SSTA contrast and OLR anomalies is statistically significant at the 95% level based on a Student's *t* test. (c) Regression of tropical (10°S to 20°N) pressure velocity (omega, positive value is ascending motion, shaded, 1,000 Pa s^{-1}) and vertical-zonal wind streamline onto the interbasin SSTA contrast in ASO.

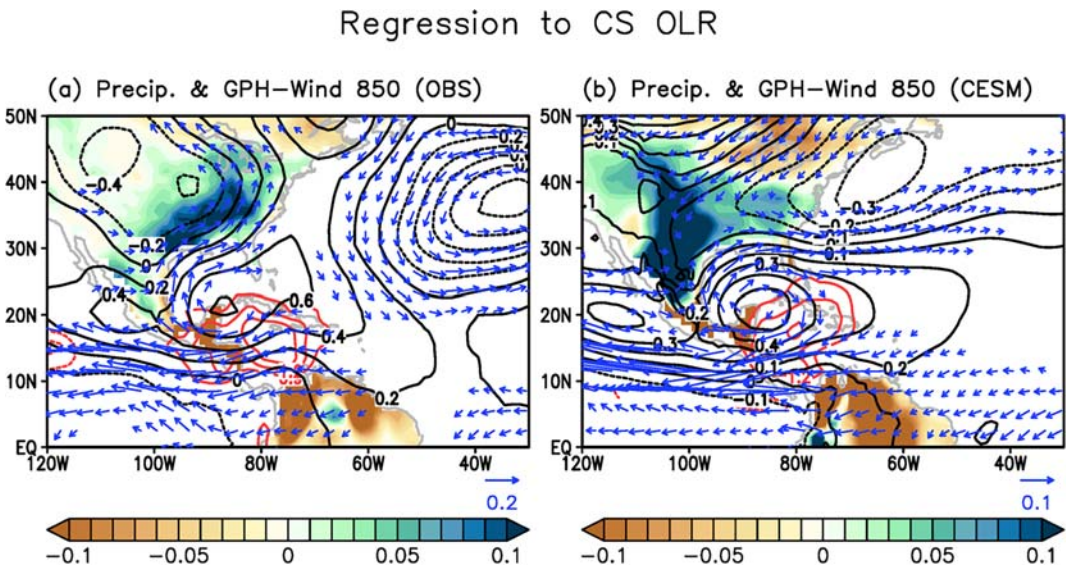

Figure 3. (a) Precipitation (shaded), wind (vectors), and geopotential height at 850 hPa (black contours) from observations and NCEP2 regressed onto CS OLR anomalies (red contours) in ASO for 40 years (1979–2018). (b) Same as (a) but derived from a 1,100 model year run from CESM-LENS.

5. Physical Mechanism Linking CS Convective Activity and U.S. Precipitation in ASO

We now investigate how CS convective activity influences U.S. precipitation in ASO. Figure 3a shows precipitation, geopotential height, and wind anomalies at 850 hPa regressed onto CS OLR anomalies in ASO. The anomalous subsidence and diabatic cooling over the CS, implied by strongly positive OLR anomalies, produce an anomalous low-level atmospheric ridge centered over the GoM, which appears to be consistent with a Gill-type response to the CS diabatic cooling (Gill, 1980). This anomalous low-level atmospheric ridge produces an anomalous low-level anticyclonic circulation, which reinforces the NALLJ over the southern United States and thus increases the moisture and heat fluxes from the GoM to the United States. Consistently, precipitation increases over the United States east of the Rockies. Therefore, we conclude that anoamlous diabatic cooling (i.e., suppressed convection) in the CS produces an anomalous low-level anticyclonic circulation to its northwest via a Gill-type response to increase the moisture and heat fluxes from the GoM to the United States, consequently increasing U.S. precipitation.

Despite these physically consistent relationships, the observational record used in this study may not be long enough to establish a robust conclusion. It is also possible that linear detrending does not completely remove the influences of anthropogenic global warming in the observational and atmospheric reanalysis products. Therefore, we carry out the same analyses using a 1,100 model year simulation derived from CESM-LENS with a constant preindustrial CO_2 level. The relationship between CS OLR anomalies and interbasin SSTAs derived from observations (Figure 2) are well simulated in CESM-LENS (Figure S3). Figure 3b shows precipitation, and geopotential height and wind anomalies at 850 hPa regressed onto the CS OLR anomalies, based on CESM-LENS. These results are very similar to those derived from the observational and atmospheric reanalysis products. The only major difference is that the center of increased U.S. precipitation shifts westward to Mexico and the south central United States. This appears to be linked to the westward extension of the anomalous low-level trough from the North Atlantic. Therefore, the results derived from CESM-LENS strongly support the conclusion that the remote influence of CS OLR anomalies on U.S. precipitation is ultimately forced by an interbasin SSTA contrast.

6. LBM Experiments

Figure 4a shows the observed geopotential height anomalies at 500 hPa regressed onto U.S. precipitation. A pair of anomalous atmospheric trough and ridge appear over North America and the GoM, respectively. As discussed in section 5, the atmospheric ridge centered in the GoM is forced by anomalous diabatic cooling in

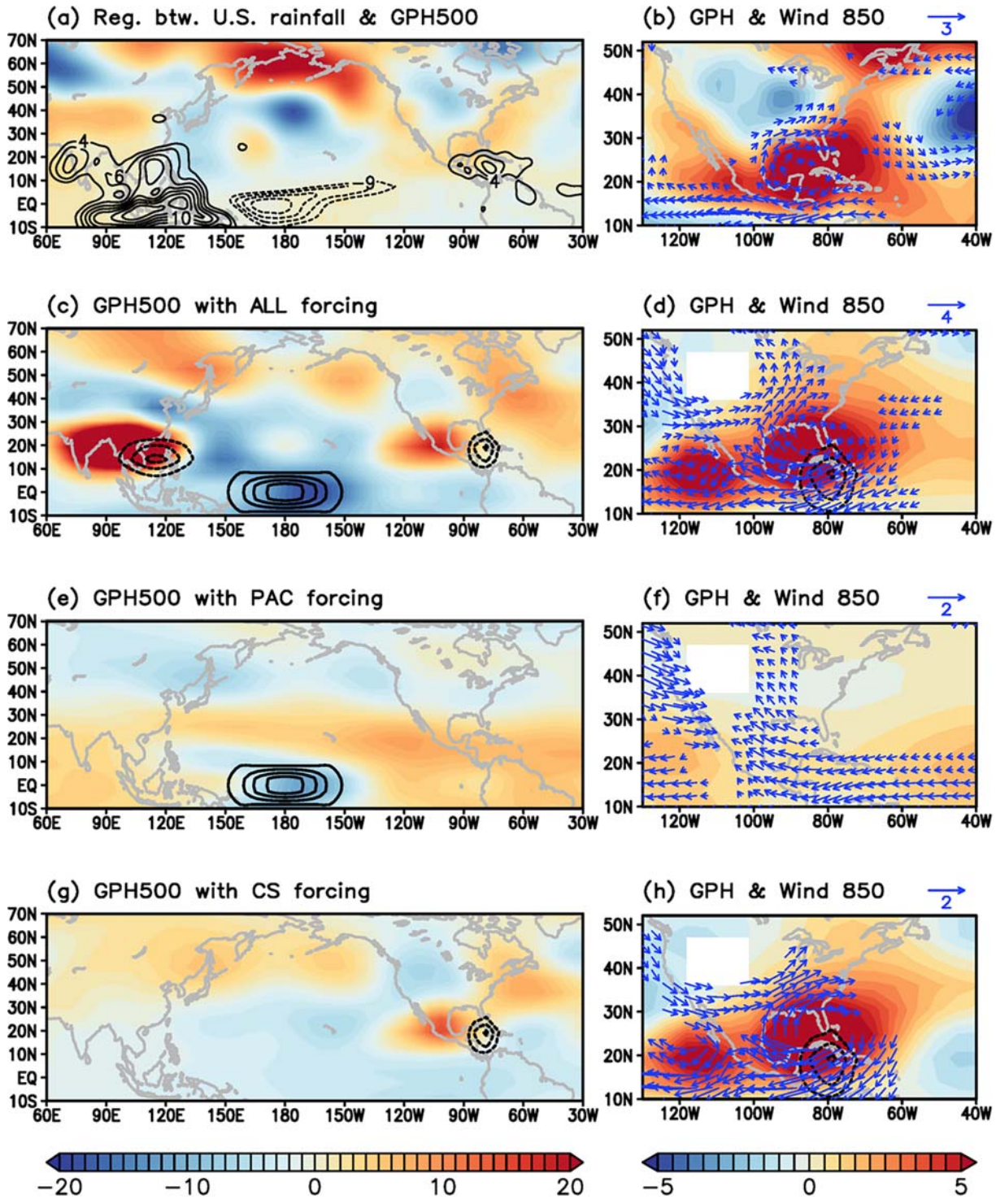

Figure 4. (a) Geopotential height at 500 hPa (shaded) and OLR anomalies (contour) regressed onto U.S. precipitation in ASO. (b) Geopotential height (shaded) and wind anomalies at 850 hPa (vectors) regressed onto U.S. precipitation in ASO. (c) Geopotential height at 500 hPa (shaded, gpm) and (d) geopotential height (shaded, gpm) and wind anomalies at 850 hPa (vectors, m s^{-1}) derived from the ALL forcing experiment. Contour lines indicate the diabatic forcing in the LBM experiment. (e and f, g and h) Same as (c) and (d), but for those derived from the PAC forcing experiment and CS forcing experiment, respectively.

the CS via a Gill-type response. Interestingly, another meridional dipole in geopotential height appears over the Bering Sea and the North Pacific. It is likely that these atmospheric circulation anomalies are extratropical Rossby waves forced by anoamlous diabatic heating over the tropical Pacific or by

anomalous diabatic cooling over the SCS. Therefore, it is also possible that anomalous diabatic heating and cooling in the tropical Pacific and SCS, through extratropical Rossby wave trains, may reinforce or interfere with the CS-forced anomalous low-level atmospheric ridge centered over the GoM and thus may also influence U.S. precipitation.

To test this possibility, we carry out four LBM experiments focusing on the roles of the three tropical regions (i.e., PAC, CS, and SCS) in producing the anomalous low-level atmospheric ridge over the GoM. The first LBM experiment is performed by prescribing anomalous diabatic heating (solid lines) over the tropical Pacific (150°E to 150°W, 10°S to 10°N) and anomalous diabatic cooling (dotted lines) over the SCS (95°E to 135°W, 10–20°N) and the CS (90–70°W, 10–20°N), as shown in Figure 4c. This experiment is referred to as the ALL forcing experiment and is designed to test whether the LBM can reproduce the observed atmospheric circulation anomalies associated with U.S. precipitation. The magnitude of anomalous diabatic heating over the tropical Pacific is set to 1.5 K day^{-1}, which is derived based on the OLR anomalies averaged over the tropical Pacific (e.g., Kim et al., 2020; Ting & Yu, 1998). Similarly, the magnitudes of anomalous diabatic cooling over the SCS and CS regions are both set to −1.0 K day^{-1}. In this and other LBM experiments, the three-dimensional background atmospheric states are prescribed using ASO fields averaged for the period of 1979–2018 and derived from NCEP2. The anomalous heating and cooling profiles are idealized to have their maximum values at midlevel near 500 hPa, with a Gaussian distribution for both vertical and horizontal directions.

Figure 4c shows the midlevel (500 hPa) geopotential height anomalies driven by the three diabatic forcings in the ALL forcing experiment. Overall, the spatial patterns of midlevel geopotential height anomalies in the ALL forcing experiment are largely consistent with those derived from NCEP2, despite differences in the amplitudes of some features. Although the anomalous low-level atmospheric trough centered over North America is weaker, the anomalous low-level atmospheric ridge over the GoM and the southwesterly wind anomalies that enhance the NALLJ are well captured in the ALL forcing experiment (Figure 4d). These results from the ALL forcing experiment suggest that anomalous diabatic heating and cooling associated with the Pacific-Atlantic SSTA contrast modulate the NALLJ, which has a strong impact on U.S. warm season precipitation.

In order to explore further which of the three diabatic forcings most strongly influences U.S. precipitation in ASO, we carry out three additional LBM experiments. In the PAC forcing experiment, only anomalous diabatic heating over the tropical Pacific is prescribed, while in the CS forcing experiment, only anomalous diabatic cooling over the CS is prescribed. In the SCS forcing experiment, only anoamlous diabatic cooling over the SCS is prescribed. In the PAC forcing experiment, a pair of anomalous cyclonic circulation feature to the northwest (10°N) and southwest (10°S) of the center of diabatic heating in the tropical Pacific (Figure 4e). The midlevel geopotential height anomalies over the Pacific and North America in this experiment are distinct from those derived from the ALL forcing experiment (Figures 4c–4f). In the SCS forcing experiment, the impact of anomalous diabatic forcing over the SCS on atmospheric circulations is very weak over North America (Text S1 and Figures S4a-b).

As shown in Figure 4g, the CS forcing experiment simulates a robust pattern of anomalous midlevel geopotential height over North America and the Atlantic Ocean, consistent with those derived from the ALL forcing experiment (Figure 4c). In particular, a midlevel atmospheric trough appears over North America and a ridge across Central America. An anomalous low-level atmospheric ridge appears over the GoM, which appears to be a Gill-type response (Gill, 1980) to the anomalous diabatic cooling over the CS judging from its position to the northwest of diabatic forcing and its strong baroclinic structure (Figure 4h). The anomalous low-level atmospheric ridge produces low-level southwesterly wind anomalies over the United States east of the Rockies. These results are consistent with our observation-based results and strongly support our hypothesis that anomalous diabatic cooling over the CS, driven by the interbasin SSTA contrast, is a key driver of atmospheric circulation anomalies that are conducive to increasing U.S. precipitation in ASO.

7. Concluding Remarks

In this study, we found that the well-recognized NASH-U.S. peak summer precipitation relationship is not applicable in late summer to midfall (ASO). Instead, the working hypothesis derived from our analysis is that the tropical Pacific-Atlantic SSTA contrast modulates convective activity in the CS in ASO. This change in

regional convection directly influences the NALLJ and thus U.S. precipitation east of the Rockies, through a Gill-type response. We further used a long-term climate model simulation (CESM-LENS) and carried out a series of LBM experiments to confirm this hypothesis.

The main conclusion of this study aligns well with several key findings from previous studies, including the positive relationship between tropical Pacific SSTAs and NALLJ (e.g., Krishnamurthy et al., 2015; Weaver et al., 2009), the negative relationship between AWP SSTAs and U.S. summer rainfall (e.g., Wang et al., 2006, 2007, 2008), and the robust relationship between CS rainfall and the Pacific-Atlantic SSTA contrast. This study integrates these key findings from previous studies to advance a consistent physical rationale that links the Pacific-Atlantic SSTA contrast, CS convective activity, and U.S. precipitation in ASO.

There remain several questions that are not extensively explored in this study. First, our study focuses on interannual time scale between 1979 and 2018. Therefore, it is not clear if the physical mechanism proposed in this study is applicable to decadal-to-centennial time scales. For instance, Liu et al. (2015) showed that the U.S. precipitation response to the Atlantic Multidecadal Oscillation (AMO) in ASO is very different from that related to interannual variability of the AWP. Therefore, it is important to explore the impact of the Pacific-Atlantic SSTA contrast on the U.S. hydrological cycle at decadal-to-centennial time scales in future works. Another important point is that AWP SSTAs are largely forced from the high-latitude North Atlantic and tropical Pacific during boreal winter and spring (e.g., Czaja et al., 2002; Enfield et al., 2006; Lee et al., 2008) but normally dissipate before peak summer. Therefore, it is not entirely clear what physical processes control or affect AWP SSTAs in ASO. Properly addressing these questions through targeted modeling and observational studies could potentially improve seasonal to decadal prediction capability for U.S. summer to fall precipitation.

Acknowledgments

We thank Renellys Perez for helpful comments and suggestions. Dongmin Kim was supported under the auspices of the Cooperative Institute for Marine and Atmospheric Studies (CIMAS), a cooperative institute of the University of Miami and NOAA, Cooperative Agreement NA10OAR4320143. This work was also supported by NOAA's Climate Program Office, Climate Variability and Predictability Program (Award GC16-207) and NOAA's Atlantic Oceanographic and Meteorological Laboratory. Monthly NOAA's interpolated OLR, ERSSTv5, and NCEP2 data were provided by NOAA Earth System Research Laboratory (ESRL) Physical Science Division (PSD) (at https://www.esrl.noaa.gov/psd/data/gridded/tables/monthly.html). CESM-LENS data were provided by NCAR (at http://www.cesm.ucar.edu/projects/community-projects/LENS).

References

Algarra, I., Eiras-Barca, J., Miguez-Macho, G., Nieto, R., & Gimeno, L. (2019). On the assessment of the moisture transport by the Great Plains low-level jet. *Earth System Dynamics*, *2019*(10), 107–119. https://doi.org/10.5194/esd-10-107-2019

Arias, P. A., Fu, R., & Mo, K. C. (2012). Decadal variation of rainfall seasonality in the North American monsoon region and its potential causes. *Journal of Climate*, *25*(12), 4258–4274. https://doi.org/10.1175/JCLI-D-11-00140.1

Bishop, D. A., Williams, A. P., Seager, R., Fiore, A. M., Cook, B. I., Mankin, J. S., et al. (2019). Investigating the causes of increased twentieth-century fall precipitation over the southeastern United States. *Journal of Climate*, *32*(2), 575–590. https://doi.org/10.1175/JCLI-D-18-0244.1

Bjerknes, J. (1969). Atmospheric teleconnections from the equatorial Pacific. *Monthly Weather Review*, *97*(3), 163–172. https://doi.org/10.1175/1520-0493(1969)097<0163:ATFTEP>2.3.CO;2

Chiang, J. C., & Sobel, A. H. (2002). Tropical tropospheric temperature variations caused by ENSO and their influence on the remote tropical climate. *Journal of Climate*, *15*(18), 2616–2631. https://doi.org/10.1175/1520-0442(2002)015<2616:TTTVCB>2.0.CO;2

Curtis, S. (2008). The Atlantic Multidecadal Oscillation and extreme daily precipitation over the US and Mexico during the hurricane season. *Climate Dynamics*, *30*(4), 343–351. https://doi.org/10.1007/s00382-007-0295-0

Czaja, A., Vaart, P. V., & Marshall, J. (2002). A diagnostic study of the role of remote forcing in tropical Atlantic variability. *Journal of Climate*, *15*(22), 3280–3290. https://doi.org/10.1175/1520-0442(2002)015<3280:ADSOTR>2.0.CO;2

Enfield, D. B., & Alfaro, E. J. (1999). The dependence of Caribbean rainfall on the interaction of the tropical Atlantic and Pacific Oceans. *Journal of Climate*, *12*(7), 2093–2103. https://doi.org/10.1175/1520-0442(1999)012<2093:TDOCRO>2.0.CO;2

Enfield, D. B., Lee, S.-K., & Wang, C. (2006). How are large Western Hemisphere warm pools formed? *Progress in Oceanography*, *70*(2-4), 346–365. https://doi.org/10.1016/j.pocean.2005.07.006

Enfield, D. B., Mestas-Nunez, A. M., & Trimble, P. J. (2001). The Atlantic Multidecadal Oscillation and its relationship to rainfall and river flows in the continental U.S. *Geophysical Research Letters*, *28*(10), 2077–2080. https://doi.org/10.1029/2000GL012745

Feng, S., Hu, Q., & Oglesby, R. J. (2011). Influence of Atlantic sea surface temperature on persistent drought in the North America. *Climate Dynamics*, *37*(3-4), 569–586. https://doi.org/10.1007/s00382-010-0835-x

Giannini, A., Cane, M. A., & Kushnir, Y. (2001). Interdecadal changes in the ENSO teleconnection to the Caribbean region and the North Atlantic Oscillation. *Journal of Climate*, *14*(13), 2867–2879. https://doi.org/10.1175/1520-0442(2001)014<2867:ICITET>2.0.CO;2

Giannini, A., Kushnir, Y., & Cane, M. A. (2000). Interannual variability of Caribbean rainfall, ENSO and the Atlantic Ocean. *Journal of Climate*, *13*(2), 297–311. https://doi.org/10.1175/1520-0442(2000)013<0297:IVOCRE>2.0.CO;2

Gill, A. E. (1980). Some simple solutions for heat-induced tropical circulation. *Quarterly Journal of the Royal Meteorological Society*, *106*(449), 447–462. https://doi.org/10.1002/qj.49710644905

Hu, Q., & Feng, S. (2008). Variation of North American summer monsoon regimes and the Atlantic Multidecadal Oscillation. *Journal of Climate*, *21*, 2373–2383.

Hu, Q., & Feng, S. (2012). AMO- and ENSO-driven summertime circulation and precipitation variations in North America. *Journal of Climate*, *25*(19), 6477–6495. https://doi.org/10.1175/JCLI-D-11-00520.1

Hu, Q., Feng, S., & Oglesby, R. J. (2011). Variations in North American summer precipitation driven by the Atlantic Multidecadal Oscillation. *Journal of Climate*, *24*(21), 5555–5570. https://doi.org/10.1175/2011JCLI4060.1

Huang, B., Thorne, P. W., Banzon, V. F., Boyer, T., Chepurin, G., Lawrimore, J. H., et al. (2017). Extended Reconstructed Sea Surface Temperature, Version 5 (ERSSTv5): Upgrades, validations, and intercomparisons. *Journal of Climate*, *30*(20), 8179–8205. https://doi.org/10.1175/JCLI-D-16-0836.1

Jones, P., & Harris, I. (2013). CRU TS3.21: Climatic Research Unit (CRU) time-series (TS) version 3.21 of high resolution gridded data of month-by-month variation in climate (January 1901 –December 2012), https://doi.org/10.5285/D0E1585D-3417-485F-87AE-4FCECF10A992

Kanamitsu, M., Ebisuzaki, W., Woollen, J., Yang, S., Hnilo, J. J., Fiorino, M., & Potter, G. L. (2002). NCEP–DOE AMIP-II Reanalysis (R-2). *Bulletin of the American Meteorological Society*, *83*(11), 1631–1644. https://doi.org/10.1175/BAMS-83-11-1631

Kay, J. E., Deser, C., Phillips, A., Mai, A., Hannay, C., Strand, G., et al. (2015). The Community Earth System Model (CESM) Large Ensemble Project: A community resource for studying climate change in the presence of internal climate variability. *Bulletin of the American Meteorological Society*, *96*(8), 1333–1349. https://doi.org/10.1175/BAMS-D-13-00255.1

Kim, D., Lee, S.-K., & Lopez, H. (2020). Madden-Julian Oscillation-induced suppression of northeast Pacific convection increases U.S. tornadogenesis. *Journal of Climate*, *33*(11), 4927–4939. https://doi.org/10.1175/JCLI-D-19-0992.1

Krishnamurthy, L., Vecchi, G. A., Msadek, R., Wittenberg, A., Delworth, T. L., & Zeng, F. (2015). The seasonality of the Great Plains low-level jet and ENSO relationship. *Journal of Climate*, *28*(11), 4525–4544. https://doi.org/10.1175/JCLI-D-14-00590.1

Lee, S.-K., Enfield, D. B., & Wang, C. (2007). What drives the seasonal onset and decay of the Western Hemisphere Warm Pool? *Journal of Climate*, *20*(10), 2133–2146. https://doi.org/10.1175/JCLI4113.1

Lee, S.-K., Enfield, D. B., & Wang, C. (2008). Why do some El Niños have no impact on tropical North Atlantic SST? *Geophysical Research Letters*, *35*, L16705. https://doi.org/10.1029/2008GL034734

Lee, S.-K., Wang, C., & Mapes, B. E. (2009). A simple atmospheric model of the local and teleconnection responses to tropical heating anomalies. *Journal of Climate*, *22*(2), 272–284. https://doi.org/10.1175/2008JCLI2303.1

Li, W., Li, L., Fu, R., Deng, Y., & Wang, H. (2011). Changes to the North Atlantic subtropical high and its role in the intensification of summer rainfall variability in the southeastern United States. *Journal of Climate*, *24*(5), 1499–1506. https://doi.org/10.1175/2010JCLI3829.1

Liebmann, B., & Smith, C. A. (1996). Description of a complete (interpolated) outgoing longwave radiation dataset. *Bulletin of the American Meteorological Society*, *77*, 1275–1277.

Lintner, B. R., & Chiang, J. C. (2007). Adjustment of the remote tropical climate to El Niño conditions. *Journal of Climate*, *20*(11), 2544–2557. https://doi.org/10.1175/JCLI4138.1

Liu, H., Wang, C., Lee, S.-K., & Enfield, D. (2015). Inhomogeneous influence of the Atlantic Warm Pool on United States precipitation. *Atmospheric Science Letters*, *16*(1), 63–69. https://doi.org/10.1002/asl2.521

Lopez, H., Lee, S.-K., Dong, S., Goni, G., Kirtman, B., Atlas, R., & Kumar, A. (2019). East Asian Monsoon as a modulator of U.S. Great Plains heat waves. *Journal of Geophysical Research: Atmospheres*, *124*, 6342–6358. https://doi.org/10.1029/2018JD030151

McCabe, G. J., Palecki, M. A., & Betancount, J. L. (2004). Pacific and Atlantic Ocean influences on multi-decadal drought frequency in the United States. *Proceedings of the National Academy of Sciences of the United States of America*, *101*(12), 4136–4141. https://doi.org/10.1073/pnas.0306738101

Misra, V., & Li, H. (2014). The seasonal climate predictability of the Atlantic Warm Pool and its teleconnections. *Geophysical Research Letters*, *41*, 661–666. https://doi.org/10.1002/2013GL058740

Misra, V., Moeller, L., Stefanova, L., Chan, S., O'Brien, J. J., Smith, T. J. III, & Plant, N. (2011). The influence of Atlantic Warm Pool on Panhandle Florida sea breeze. *Journal of Geophysical Research*, *116*, D00Q06. https://doi.org/10.1029/2010JD015367

Mo, K. C., & Schemm, J. E. (2008). Drought and persistent wet spells over the United States and Mexico. *Journal of Climate*, *21*(5), 980–994. https://doi.org/10.1175/2007JCLI1616.1

Mo, K. C., Schemm, J. K. E., & Yoo, S. H. (2009). Influence of ENSO and the Atlantic Multidecadal Oscillation on drought over the United States. *Journal of Climate*, *22*(22), 5962–5982. https://doi.org/10.1175/2009JCLI2966.1

Nigam, S., Guan, B., & Ruiz-Barradas, A. (2011). Key role of the Atlantic Multidecadal Oscillation in 20th century drought and wet periods over the Great Plains. *Geophysical Research Letters*, *38*, L16713. https://doi.org/10.1029/2011GL048650

Schubert, S. D., Gutzler, H., Wang, L., Dai, A., Delworth, T., Deser, C., et al. (2009). A US CLIVAR project to assess and compare the responses of global climate models to drought-related SST forcing patterns: Overview and results. *Journal of Climate*, *22*(19), 5251–5272. https://doi.org/10.1175/2009JCLI3060.1

Seager, R. (2007). The turn of the century North American drought: Global context, dynamics, and past analogs. *Journal of Climate*, *20*(22), 5527–5552. https://doi.org/10.1175/2007JCLI1529.1

Song, F., Leung, L. R., Lu, J., & Dong, L. (2018a). Seasonally-dependent responses of subtropical highs and tropical rainfall to anthropogenic warming. *Nature Climate Change*, *8*(9), 787–792. https://doi.org/10.1038/s41558-018-0244-4

Song, F., Leung, L. R., Lu, J., & Dong, L. (2018b). Future changes in seasonality of the North Pacific and North Atlantic subtropical highs. *Geophysical Research Letters*, *45*, 11,959–11,968. https://doi.org/10.1029/2018GL079940

Spence, J. M., Taylor, M. A., & Chen, A. A. (2004). The effect of concurrent sea-surface temperature anomalies in the tropical Pacific and Atlantic on Caribbean rainfall. *International Journal of Climatology*, *24*(12), 1531–1541. https://doi.org/10.1002/joc.1068

Sutton, R. T., & Hodson, D. L. R. (2005). Atlantic Ocean forcing of North American and European summer climate. *Science*, *309*(5731), 115–118. https://doi.org/10.1126/science.1109496

Ting, M., & Wang, H. (1997). Summertime US precipitation variability and its relation to Pacific sea surface temperature. *Journal of Climate*, *10*(8), 1853–1873. https://doi.org/10.1175/1520-0442(1997)010<1853:SUSPVA>2.0.CO;2

Ting, M., & Yu, L. (1998). Steady response to tropical heating in wavy linear and nonlinear baroclinic models. *Journal of the Atmospheric Sciences*, *55*(24), 3565–3582. https://doi.org/10.1175/1520-0469(1998)055<3565:SRTTHI>2.0.CO;2

Wang, C., Deser, C., Yu, J. Y., Di Nezio, P., & Clement, A. (2017). El Niño and Southern Oscillation (ENSO): A review. In P. Glynn, D. Manzello, & I. Enochs (Eds.), *Coral reefs of the eastern tropical Pacific. Coral reefs of the world* (4, 85–106). Dordrecht: Springer. https://doi.org/10.1007/978-94-017-7499-4_4

Wang, C., & Enfield, D. B. (2001). The tropical Western Hemisphere Warm Pool. *Geophysical Research Letters*, *28*(8), 1635–1638. https://doi.org/10.1029/2000GL011763

Wang, C., Enfield, D. B., Lee, S. -K., & Landsea, C. (2006). Influences of the Atlantic warm pool on Western Hemisphere summer rainfall and Atlantic hurricanes. *Journal of Climate*, *19*(12), 3011–3028. https://doi.org/10.1175/JCLI3770.1

Wang, C., & Lee, S. -K. (2007). Atlantic warm pool, Caribbean low-level jet, and their potential impact on Atlantic hurricanes. *Geophysical Research Letters*, *34*, L02703. https://doi.org/10.1029/2006GL028579

Wang, C., Lee, S.-K., & Enfield, D. B. (2008). Climate response to anomalously large and small Atlantic warm pools during the summer. *Journal of Climate*, *21*(11), 2437–2450. https://doi.org/10.1175/2007JCLI2029.1

Watanabe, M., & Kimoto, M. (2000). Tropical-extratropical connection in the Atlantic atmosphere-ocean variability. *Geophysical Research Letters*, *26*, 2247–2250.

Weaver, S. J., Schubert, S., & Wang, H. (2009). Warm season variations in the low-level circulation and precipitation over the central United States in observations, AMIP simulations, and idealized SST experiments. *Journal of Climate*, *22*(20), 5401–5420. https://doi.org/10.1175/2009JCLI2984.1

Wei, W., Li, W., & Deng, Y. (2019). Intraseasonal variation of the summer rainfall over the southeastern United States. *Climate Dynamics*, *53*(1-2), 1171–1183. https://doi.org/10.1007/s00382-018-4345-6

Geophysical Research Letters

Supporting Information for

On the role of Pacific - Atlantic SST contrast and associated Caribbean Sea Convection in August-October U.S. regional rainfall variability

Dongmin Kim[1,2*], Sang-Ki Lee[2], Hosmay Lopez[2], Gregory R. Foltz[2], Vasubandhu Misra[3] and Arun Kumar[4]

[1]Cooperative Institute for Marine and Atmospheric Studies, University of Miami, Miami, FL
[2]Atlantic Oceanographic and Meteorological Laboratory, NOAA, Miami, FL
[3]Center for Ocean-Atmospheric Prediction Studies, Florida State University
[4]Climate Prediction Center, NOAA, College Park, MD

Contents of this file

Introduction

This supporting information provides Text S1, Tables S1-S2 and Figures S1-S4. Text S1 addresses the result from SCS experiment in section 6. Tables S1 and S2 provides correlation coefficient among the Atlantic and Pacific SSTAs, Caribbean Sea (CS) convective activity and U.S. precipitation during August-October (ASO) and June-August (JJA), respectively. Figure S1 shows the spatial patterns of correlation between U.S. precipitation and sea surface temperate (SST) and outgoing longwave radiation (OLR). Figure S2 shows the partial correlation of OLR anomalies onto the tropical Pacific SST and the Atlantic warm pool SST indices. Figure S3 shows the regression of SST onto CS OLR anomalies and vertical wind profiles over the tropic onto the interbasin SST contrast. Figure S4 shows the geopotential height at 500 hPa, 850 hPa and low-level wind anomalies derived from the South China Sea (SCS) forcing experiment in LBM.

Text S1.

As shown in Figure S4a, the SCS forcing experiment produces strong positive mid-level geopotential height anomalies over the Bay of Bengal in response to diabatic cooling over the SCS. The spatial patterns of anomalous mid-level geopotential height over the North Pacific are similar to those derived from the ALL forcing experiment. However, an anomalous low-level anticyclonic circulation appears over North America and an anomalous low-level cyclonic circulation over the CS (Figure S4b). These patterns are nearly opposite to those derived from the ALL forcing experiment and NCEP2, suggesting that the anomalous diabatic cooling over the SCS does not explain the strengthened NALLJ in the ALL forcing experiment.

Table S1. The correlation coefficients for combinations of Atlantic warm pool SSTAs (AWP SSTA; 80°W –40°W, 10°N – 25°N), tropical Pacific SSTAs (PAC SST; 160°E – 160°W, 0° – 10°N), normalized interbasin SSTA contrast (PAC SST – AWP SST), OLR anomalies over the Caribbean Sea (CS OLR; 90°W – 70°W, 10°N – 20°N) and U.S. precipitation (90°W – 70°W, 30°N – 40°N) during ASO. Stars (*) and bold numbers indicate that correlation coefficients are statistically significant at the 95% and 99% levels based on a Student's t-test, respectively.

	AWP SST	PAC SST	Interbasin SST	CS OLR	U.S rainfall
AWP SST	1	-0.01	-0.58*	-0.23	-0.35*
PAC SST		1	**0.80***	**0.60***	0.31*
Interbain SST			1	**0.63***	0.39*
CS OLR				1	0.45*
U.S rainfall					1

Table S2. This table is the same as Table S1 but for JJA.

	AWP SST	PAC SST	Interbain SST	CS OLR	U.S rainfall
AWP SST	1	-0.01	-0.74*	-0.54*	-0.19
PAC SST		1	**0.79***	0.32	0.09
Interbain SST			1	0.55*	0.18
CS OLR				1	0.25
U.S rainfall					1

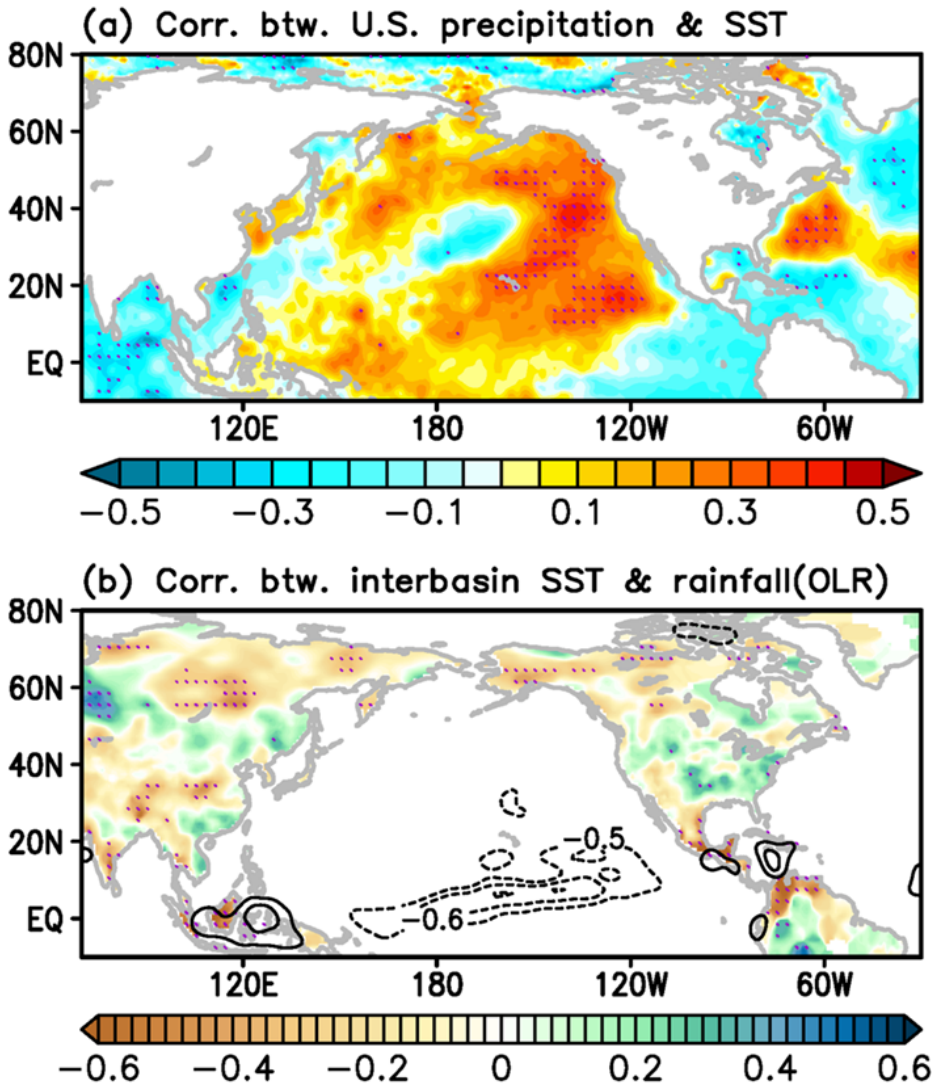

Figure S1. (a) Correlation between U.S. precipitation (90°W – 70°W, 30°N – 40°N) and SSTA in JJA for 40 years (1979-2018). (b) Correlation between interbasin SSTA contrast and precipitation in JJ (shaded). The contour lines show the correlation between the interbasin SSTA contrast and OLR anomalies in JJA. Purple dotted areas are statistically significant at the 95% level based on a Student's t-test.

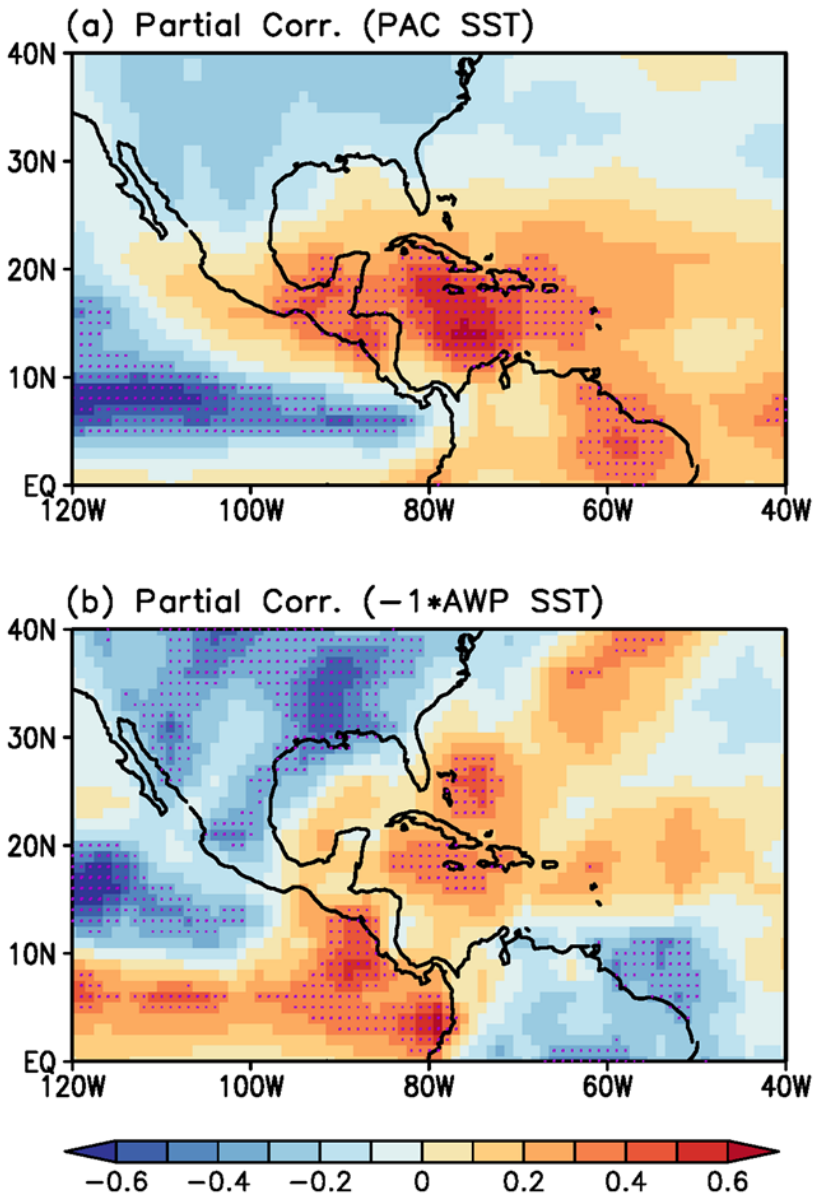

Figure S2. Partial correlation of OLR anomalies (shading) to (a) PAC SST and (b) AWP SST indices during 1979-2018. To help visual comparison, the sign of AWP SST index is reversed. Purple dotted areas in (b) are statistically significant at the 95% level based on a Student's t-test.

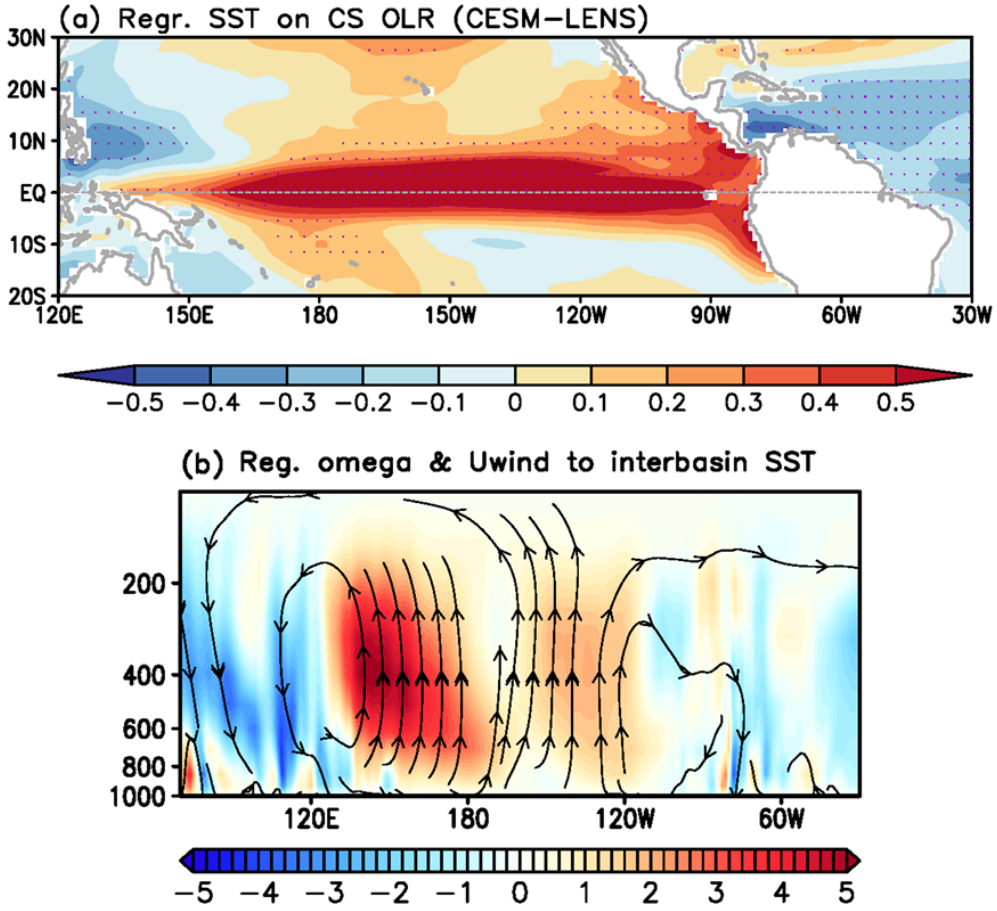

Figure S3. (a) Regression coefficients of SSTAs (shade) onto CS OLR anomalies in ASO derived from 1,100-year CESM-LENS. Purple dotted areas are statistically significant at the 95% level based on a Student's t-test. (b) Regression of tropical (10°S-20°N) pressure velocity (omega, positive value is ascending motion, shaded, 1000 Pa s-1) and vertical-zonal wind profile (streamline) onto the interbasin SSTA contrast derived from CESM-LENS.

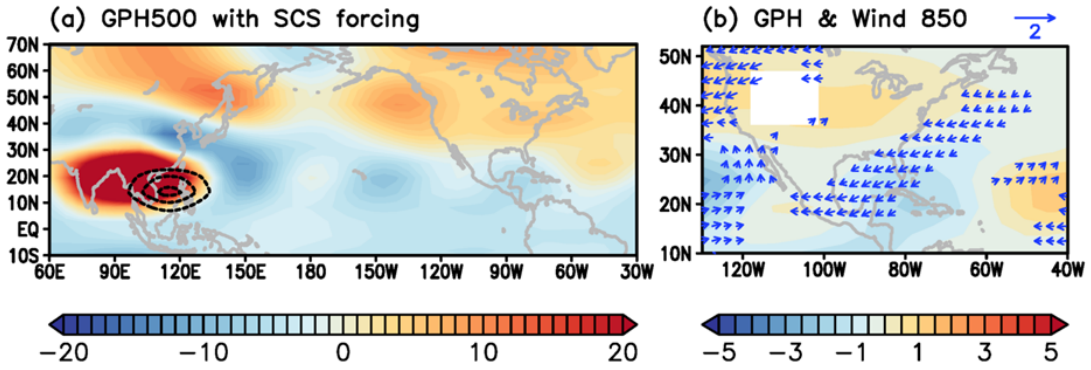

Figure S4. (a) Geopotential height at 500 hPa (shaded, gpm) and (b) geopotential height (shaded, gpm) and wind anomalies at 850 hPa (vectors, m s-1) derived from the SCS forcing experiment. Contour lines indicate the diabatic forcing in the LBM experiment.